Nonlocal viscosity kernel of mixtures

Ben Smith
Faculty of Engineering and Industrial Sciences, Swinburne University of Technology, PO Box 218, Hawthorn, Victoria 3122, Australia

J. S. Hansen*
Danish National Research Foundation Centre "Glass and Time," IMFUFA, Department of Sciences, Systems and Models, Roskilde University, PO Box 260, DK-4000 Roskilde, Denmark

B. D. Todd†
Mathematics Discipline, Faculty of Engineering and Industrial Sciences, and Centre for Molecular Simulation, Swinburne University of Technology, PO Box 218, Hawthorn, Victoria 3122, Australia
(Received 20 October 2011; revised manuscript received 21 December 2011; published 21 February 2012)

In this Brief Report we investigate the multiscale hydrodynamical response of a liquid as a function of mixture composition. This is done via a series of molecular dynamics simulations in which the wave-vector-dependent viscosity kernel is computed for three mixtures, each with 7–15 different compositions. We observe that the viscosity kernel is dependent on composition for simple atomic mixtures for all the wave vectors studied here; however, for a molecular mixture the kernel is independent of composition for large wave vectors. The deviation from ideal mixing is also studied. Here it is shown that the Lorentz-Berthelot interaction rule follows ideal mixing surprisingly well for a large range of wave vectors, whereas for both the Kob-Andersen and molecular mixtures large deviations are found. Furthermore, for the molecular system the deviation is wave-vector dependent such that there exists a characteristic correlation length scale at which the ideal mixing goes from underestimating to overestimating the viscosity.

DOI: 10.1103/PhysRevE.85.022201 PACS number(s): 66.20.Ej, 47.11.Mn

Hydrodynamics on very small length scales has become an important research area because it is believed to hold the key to understanding the many different phenomena observed in nanofluidic devices. Recent studies [1,2] have shown that the spatial correlations in the fluid reduce the shear stress compared to the stress predicted via a local response function. The nonlocal response is defined via generalized hydrodynamics [3], in which the response function is a wave-vector-dependent quantity. The wave-vector-dependent viscosity, i.e., the viscosity kernel, accounts for the momentum flux due to a nonzero strain rate. It has been evaluated for one-component fluids through molecular dynamics simulations and it was found that it follows a simple functional form reasonably well for atomic, diatomic, and polymer fluids [3–6]. The wave-vector-dependent viscosity kernel has been predicted by mode-coupling theory [7]; however, the theoretical predictions do not agree with the data from simulations [3,4]. Nevertheless, at present, the effect of the multiscale response is understood fairly well for a range of simple single-component fluids [3–6] and glasses [8,9].

In microscale and nanoscale devices usually multicomponent mixtures are transported around very narrow tubes. For example, in electro-osmosis ions are added to the fluid and will act as an actuator under appropriate conditions [10]. Thus the small-scale hydrodynamical response of multicomponent systems is of importance. In order to investigate this for two-component mixtures we evaluate the viscosity kernel for three different simple-model two-component mixtures using molecular dynamics. These are (i) a Kob-Andersen (KA) mixture [11], (ii) a Lennard-Jones (LJ) mixture using the Lorentz-Berthelot interaction rule, and (iii) a molecular mixture [12]. Mixtures (i) and (ii) thus represent atomic fluids, where only the interactions between unlike particles are different, and mixture (iii) is a simple molecular mixture that we expect to have a different hydrodynamical response compared to the atomic ones.

In all the simulations the particles interact through the Lennard-Jones cut and shifted potential $U_{\mathrm{LJ}}(r_{ij}) = 4\epsilon[(\sigma/r_{ij})^{12} - (\sigma/r_{ij})^{6}] - U(r_c)$ for $r_{ij} \leqslant r_c$, where r_{ij} is the distance between particle i and j, σ is a length scale, ϵ is an energy scale, r_c is the interaction range (cutoff), and $U(r_c)$ is the unshifted potential at r_c. The values of σ and ϵ are different for the KA and LJ mixtures depending on the pair of particles that interact (see Table I).

The cutoff radius is set to $r_c = 2.5\sigma$ for the KA and LJ mixtures and $r_c = 2^{1/6}\sigma$ for the molecular system. The latter is also referred to as the Weeks-Chandler-Andersen pair potential [13]. In the molecular mixture the particles (or beads) are bonded via the finite extensible nonlinear elastic potential [12] $U_{\mathrm{FENE}} = -kR_0\ln[1 - (r_{ij}/R_0)^2]/2$, where $k = 30\epsilon/\sigma^2$ and $R_0 = 1.5\sigma$. It is composed of two types of molecules: one with two beads, component B, and one with ten beads, component A. In what follows we give all quantities in terms of Lennard-Jones reduced units, for example, reduced distance $r^*_{ij} = r_{ij}/\sigma$ and number density $\rho^* = \rho\sigma^3$. For simplicity of notation, we will hereafter omit the asterisk.

*jschmidt@ruc.dk
†btodd@swin.edu.au

TABLE I. List of the Kob-Andersen and Lennard-Jones parameters used in this work.

Parameter	Kob-Andersen	Lennard-Jones
$\epsilon_{AA}/\epsilon_{AA}$	1	1
$\epsilon_{BB}/\epsilon_{AA}$	1/2	1/2
$\epsilon_{AB}/\epsilon_{AA}$	0.8	$\sqrt{1/2}$
σ_{AA}/σ_{AA}	1	1
σ_{BB}/σ_{AA}	0.88	0.88
σ_{AB}/σ_{AA}	0.8	0.94

The simulations are carried out at an average reduced pressure of $p = 1$ and temperature $T = 2.5$, which ensures that no phase separation takes place and that the system is homogeneous. The target pressure was obtained via an anisotropic Berendsen barostat [14] such that the simulation box was varied in the x direction only. The temperature was controlled via a Nosé-Hoover thermostat [15,16].

The expression for the wave-vector-dependent viscosity can be found from the generalized Navier-Stokes equation and is given in terms of the transverse-momentum current-density autocorrelation function $\widetilde{C}_\perp(k,t)$ [17,18],

$$\eta(k,\omega) = \frac{\rho}{k^2}\frac{\widetilde{C}_\perp(k,t=0) - i\omega\widehat{C}_\perp(k,\omega)}{\widehat{C}_\perp(k,\omega)}, \qquad (1)$$

where ρ is the mass density; k is the z component the wave vector, i.e., $k = 2\pi n/L_z$, $n = 1,2,\ldots$, where L_z is the simulation box length in the z direction; and $\widetilde{C}_\perp(k,t) = \langle \widetilde{J}_y(k,0)\widetilde{J}_y(k,t)\rangle/V$. The transverse-momentum density is here defined via $\widetilde{J}_y(k,t) = \sum_{i=1}^{N} m_i v_{y,i}(t)e^{ikz_i}$, where m_i and $v_{y,i}$ are the center of mass and center-of-mass velocity of the molecule or particle i. The term $\widehat{C}_\perp(k,\omega)$ is the Fourier-Laplace transform of $\widetilde{C}_\perp(k,t)$, that is, $\widehat{C}_\perp(k,\omega) = \int_0^\infty \widetilde{C}_\perp(k,t)e^{i\omega t}dt$. Also note that because the barostat is anisotropic and only varies the simulation box in the x direction, L_z is constant.

In Fig. 1 we have plotted the viscosity kernel data in the limit $\omega \to 0$ for different composition fractions of A, $x_A = N_A/N_t$, where N_A is the number of A particles and N_t is the total number of particles. Recall that in the molecular system we label the ten-bead molecule A. From Fig. 1 it is observed that for the KA and LJ mixtures the hydrodynamical response is dependent on the exact composition for all length scales studied here. This is not the case for the molecular system: Here the fluid response is largely independent of the fluid composition for sufficiently large wave vectors. The reason behind this is that the molecular fluid experiences the same physical environment at the small lengths scales no matter the composition. We believe this is linked to the fact that the bead-bead intramolecular and intermolecular particle interactions are the same and therefore no distinct microscale structures are present at these length scales. The scale at which this occurs is here denoted by the characteristic correlation length scale and we shall return to this later. We also point out that no characteristic correlation length is observed for the atomic systems where the atom interactions are dependent on the type.

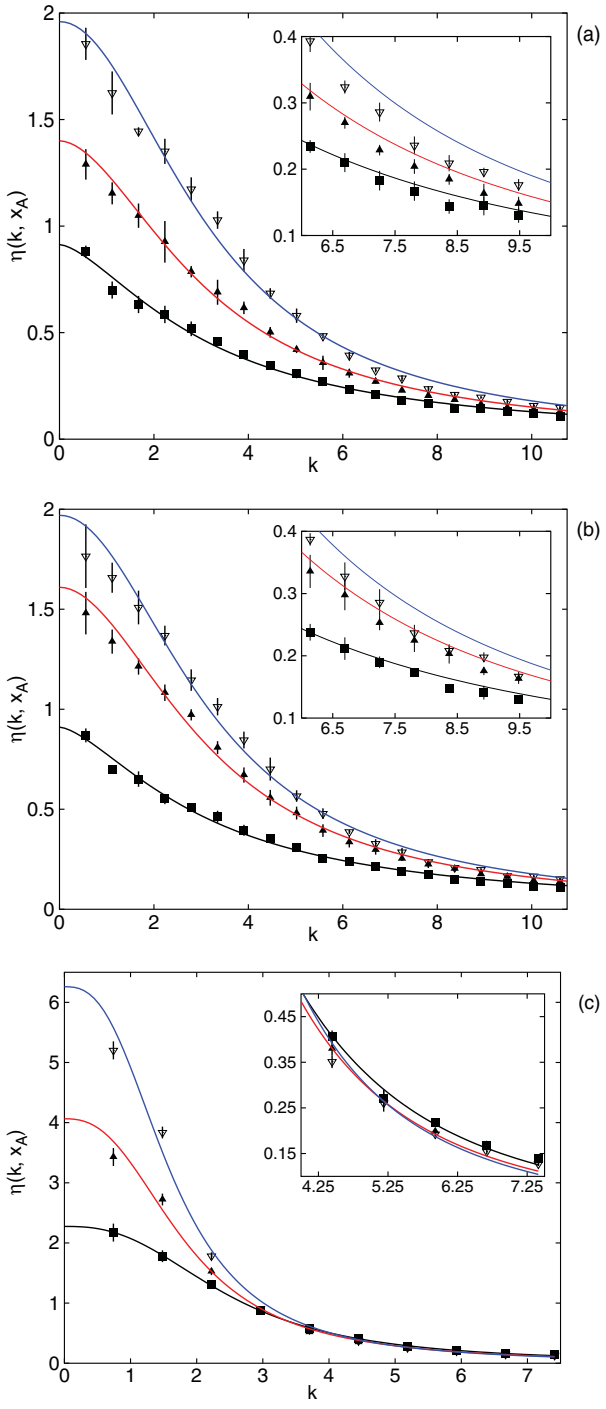

FIG. 1. (Color online) Viscosity kernel data (symbols) for (a) the Kob-Andersen mixture, (b) the Lennard-Jones mixture, and (c) the molecular mixture. (a) and (b) $x_A = 0$ (solid squares), 0.8 (upward-pointing solid triangles), and 1 (downward-pointing open triangles). (c) $x_A = 0$ (solid squares), 0.25 (upward-pointing solid triangles), and 1 (downward-pointing open triangles). The error bars are the standard error. Lines represent the best fit of the data to Eq. (2). The insets depict the kernels for large k.

In order to decrease the statistical error in the further analysis we fit the data to a Lorentzian functional form

$$\eta(k,x_A) = \frac{\eta_0(x_A)}{1+\alpha k^\beta}, \qquad (2)$$

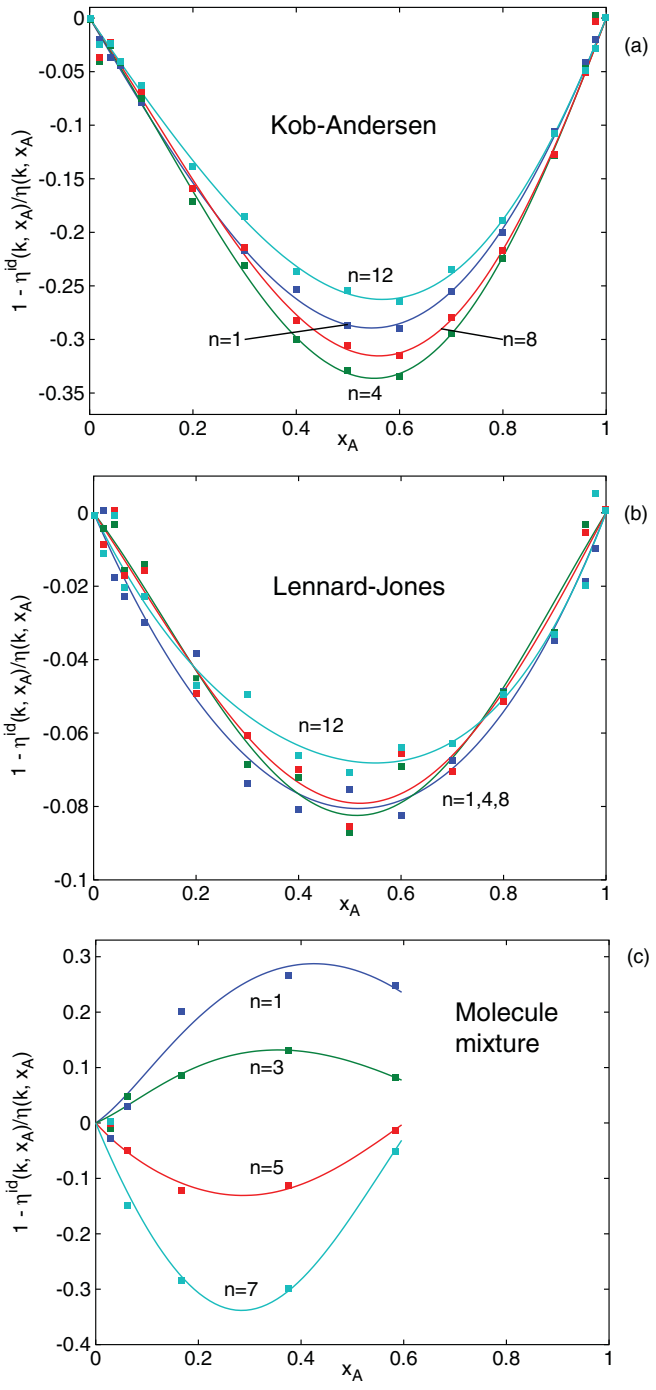

FIG. 2. (Color online) Relative excess viscosity as a function of composition and wave number n. (a) The Kob-Andersen mixture, (b) the Lennard-Jones mixture, and (c) the molecular mixture. Lines are the corresponding fits using Eq. (4). Note that the wave number is given via the definition of the wave vector $k = 2\pi n/L_z$.

where α and β are fitting parameters that depend on the fraction of A, x_A, and $\eta_0(x_A)$ is the zero-frequency viscosity for $k = 0$. Equation (2) has been shown to fit viscosity kernel data well for a range of different noncharged single-component fluids [4–6] and is here extended to include the composition dependence. The result of the fitting is depicted in Fig. 1, where the insets show the data and the fits for large values of k. It is seen that Eq. (2) fits data well for all three systems; however, we stress that the agreement is not satisfactory for large values of k in the cases of Kob-Andersen and Lennard-Jones mixtures. With this in mind, we will from now on use the fitted values of the viscosity kernels rather than the raw molecular dynamics data.

We can define the k-dependent excess viscosity as

$$\eta^E(k,x_A) = \eta(k,x_A) - \eta^{\mathrm{id}}(k,x_A), \tag{3}$$

where $\eta^{\mathrm{id}}(k,x_A)$ is the ideal part of the viscosity kernel given by an Arrhenius-type mixing rule [19,20] $\eta^{\mathrm{id}}(k,x_A) = \eta_A(k)^{x_A}\eta_B(k)^{1-x_A}$, where $\eta_A(k)$ and $\eta_B(k)$ are the viscosity kernels of pure A and B, respectively. The excess viscosity has been fitted to various simple mixing models including the Kendall-Monroe model [20], the Lederer model (see, for example, Ref. [21]), and an extended version of the Grundberg-Nissan model [22]. We have found that the fourth-order McAllister model [23] fit the data best. This model was originally written in terms of the dynamical viscosity $\nu = \eta/\rho$ and may readily be extended to include the wave-vector dependence, that is,

$$\begin{aligned}
&\ln\nu(k,x_A)\\
&\quad = x_A^4\ln[\nu_A(k)] + 4x_A^3x_B\ln[M_{31}(k)] + 6x_A^2x_B^2\ln[M_{22}(k)]\\
&\qquad + 4x_Ax_B^3\ln[M_{13}(k)] + x_B^4\ln[\nu_B(k)] - \ln(x_A + x_Bm_r)\\
&\qquad + 4x_A^3x_B\ln\left(\frac{3+m_r}{4}\right) + 6x_A^2x_B^2\ln\left(\frac{1+m_r}{2}\right)\\
&\qquad + 4x_Ax_B^3\ln\left(\frac{1+3m_r}{4}\right) + x_B^4\ln(m_r),
\end{aligned} \tag{4}$$

where m_r is given by m_B/m_A and M_{31}, M_{22}, and M_{13} are the wave-vector-dependent McAllister coefficients. Recall that since we study binary mixtures, $x_B = 1 - x_A$. From Eq. (4) one can easily extract the McAllister excess kinematic viscosity using M_{31}, M_{22}, and M_{13} as fitting parameters. Rather than comparing the absolute excess viscosities, we compare the relative deviation from ideal mixing using

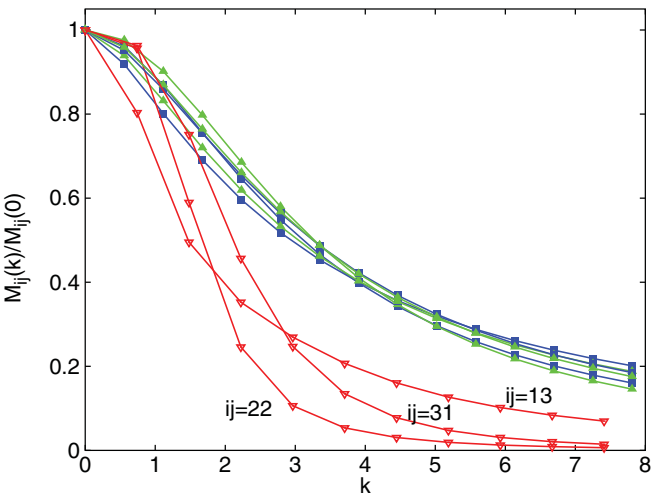

FIG. 3. (Color online) McAllister coefficients as functions of wave vector k. Solid squares represent the results for the Kob-Andersen mixture, upward-pointing solid triangles represent the Lennard-Jones mixture, and downward-pointing open triangles represent the molecular mixture. Lines serve as a guide to the eye.

$\eta^E(k,x_A)/\eta(k,x_A) = 1 - \eta^{\mathrm{id}}(k,x_A)/\eta(k,x_A)$. This is done in Fig. 2.

We note that the normalized excess viscosity is a measure of the relative deviation from ideal mixing. First, it is observed that the KA and molecular mixtures feature large deviations from the ideal mixing compared to the LJ mixture, that is, the Lorentz-Berthelot interaction rule features a more Arrhenius-like behavior compared to the KA interaction rule for all wavelengths. Second, for the KA and LJ mixtures the relative excess viscosity varies very little with respect to wave vector, meaning that the relative difference between the ideal mixing response function and the actual response is weakly wave-vector dependent. For the molecular mixture [Fig. 2(c)] we observe that the relative excess viscosity is strongly wave-vector dependent. This was also indicated in Fig. 1(c), where it was discussed that the kernel is independent of composition for large k. To high-light this special behavior further we have plotted the McAllister coefficients as functions of wave vector in Fig. 3. We see that $M_{ij}(k)/M_{ij}(0), \{ij\} = \{31\}, \{22\}$, and $\{13\}$, fall on a master curve in the case of KA and LJ mixtures; thus the three functions $M_{ij}(k)$ may be described by a single function that is directly proportional to any of the three $M_{ij}(k)$. For the molecular mixture this is not the case, due to the characteristic correlation length scale featured in this system. Note that all the McAllister coefficients follow a Lorentzian form [see Eq. (2)], but for the molecular mixture the parameters α and β are dependent on the index $\{ij\}$.

In this Brief Report we have investigated the multiscale hydrodynamical viscous response as a function of fluid composition. This was done through the viscosity kernel that was computed via equilibrium molecular dynamics simulations. We studied three different mixtures, namely, (i) a Kob-Andersen mixture, (ii) a Lennard-Jones mixture using the Lorentz-Berthelot interaction rule, and (iii) a molecular mixture. We observed that the viscosity kernel is independent of the wave vector for large wave vectors in the case of the molecular system, that is, the hydrodynamical response at these length scales is independent of the composition. This was not the case for the simple Kob-Andersen and Lennard-Jones mixtures. The deviation from ideal mixing is small in the case of the Lennard-Jones mixture, i.e., the Lorentz-Berthelot interaction rule agrees reasonably well with the predictions from ideal mixing for all wave vectors studied here; the maximum deviation is around 8%. This was not the case for Kob-Andersen and molecular mixtures, where the deviations can be as large as 35%. Finally, the relative deviation from ideal mixing is relatively wave-vector independent in the case of the Kob-Andersen and Lennard-Jones mixtures. For the molecular mixture this deviation shows a strong wave-vector dependence since the ideal mixing rule does not predict the largely composition-independent behavior of the kernel [Fig. 1(c)]. The length scale at which the viscous response is composition independent will likely vary with the model chosen; we shall leave an in depth investigation of this to future studies.

J.S.H. wishes to acknowledge Lundbeckfonden for supporting this work as a part of Grant No. R49-A5634. The authors also wish to thank Professor Peter J. Daivis for useful comments.

[1] B. D. Todd, J. S. Hansen, and P. J. Daivis, Phys. Rev. Lett. **100**, 195901 (2008).
[2] B. D. Todd and J. S. Hansen, Phys. Rev. E **78**, 051202 (2008).
[3] W. E. Alley and B. J. Alder, Phys. Rev. A **27**, 3158 (1983).
[4] J. S. Hansen, P. J. Daivis, K. P. Travis, and B. D. Todd, Phys. Rev. E **76**, 041121 (2007).
[5] R. M. Puscasu, B. D. Todd, P. J. Daivis, and J. S. Hansen, J. Phys. Condens. Matter **22**, 195105 (2010).
[6] R. M. Puscasu, B. D. Todd, P. J. Daivis, and J. S. Hansen, Phys. Rev. E **82**, 011801 (2010).
[7] E. Leutheusser, J. Phys. C **15**, 2801 (1982).
[8] A. Furukawa and H. Tanaka, Phys. Rev. Lett. **103**, 135703 (2009).
[9] R. M. Puscasu, B. D. Todd, P. J. Daivis, and J. S. Hansen, J. Chem. Phys. **133**, 144907 (2010).
[10] H. Bruus, *Theoretical Microfluidics* (Oxford University Press, Oxford, 2008).
[11] W. Kob and H. C. Andersen, Phys. Rev. Lett. **73**, 1376 (1994).
[12] K. Kremer and G. S. Grest, J. Chem. Phys. **92**, 5057 (1990).
[13] J. D. Weeks, D. Chandler, and H. C. Andersen, J. Chem. Phys. **54**, 5237 (1971).
[14] H. J. C. Berendsen, J. P. M. Postma, W. F. van Gunsteren, A. DiNola, and J. R. Haak, J. Chem. Phys. **81**, 3684 (1984).
[15] S. Nosé, Mol. Phys. **52**, 255 (1984).
[16] W. G. Hoover, Phys. Rev. A **31**, 1695 (1985).
[17] J. P. Hansen and I. R. McDonald, *Theory of Simple Liquids* (Academic, Amsterdam, 2006).
[18] B. J. Palmer, Phys. Rev. E **49**, 359 (1994).
[19] S. Z. Arrhenius, Z. Phys. Chem. **1**, 285 (1887).
[20] J. Kendall and K. P. Monroe, J. Am. Chem. Soc. **43**, 115 (1921).
[21] E. L. Lederer, Nature (London) **139**, 27 (1931).
[22] L. Grundberg and A. H. Nissan, Nature (London) **164**, 799 (1949).
[23] R. A. McAllister, AIChE J. **6**, 427 (1960).